

Plasma Biomarkers in a Mouse Model of Preterm Labor

QING YANG, JOHN C. WHITIN, XUEFENG BRUCE LING, NIHAR R. NAYAK, HARVEY J. COHEN, JOSEPH JIN,
JAMES SCHILLING, TOM TO-SANG YU, AND ASHIMA MADAN

Departments of Pediatrics [Q.Y., J.C.W., X.B.L., H.J.C., J.J., J.S., T.T.-S.Y., A.M.], and Obstetrics and Gynecology [N.N.], Stanford University, Stanford, California 94305

ABSTRACT: Preterm labor (PTL) is frequently associated with inflammation. We hypothesized that biomarkers during pregnancy can identify pregnancies most at risk for development of PTL. An inflammation-induced mouse model of PTL was used. Surface-enhanced laser desorption/ionization time-of-flight mass spectrometry was used to analyze and compare the plasma protein (PP) profile between CD-1 mice injected intrauterine with either lipopolysaccharide (LPS) or PBS on d 14.5 of gestation. The median differences of normalized PP peaks between the two groups were determined using the Mann-Whitney *U* test and the false discovery rate. In a second series of experiments, both groups of mice were injected with a lower dose of LPS. A total of 1665 peaks were detected. Thirty peaks were highly differentially expressed ($p < 0.0001$) between the groups. Two 11 kDa protein peaks were identified by MALDI-TOF/TOF-MS and confirmed to be mouse serum amyloid A (SAA) 1 and 2. Plasma SAA2 levels were increased in LPS-treated animals compared with controls and in LPS-treated animals that delivered preterm vs. those that delivered at term. SAA2 has the potential to be a plasma biomarker that can identify pregnancies at risk for development of PTL. (*Pediatr Res* 66: 11–16, 2009)

Preterm birth is the most important cause of neonatal morbidity and mortality in the United States (1–3). Despite several interventions including use of various tocolytics, antibiotics, and monitoring uterine contractions the incidence of preterm birth in the United States has not decreased in the past few decades and is currently at 12.7% (4,5) (Births. Preliminary data for 2005 <http://www.cdc.gov/nchs/>). More recently, the use of progesterone has been shown to be effective in prevention of preterm labor (PTL) in a select group of women. However, the mechanism by which this occurs is still unknown (6,7). One of the problems in preventing PTL is our inability to accurately identify which pregnancies are most likely to be complicated by PTL (8). Detection of a biomarker during pregnancy may assist in identifying an at risk population of pregnant women in whom a particular treatment can be studied. It can also help us gain important insights into the molecular pathways resulting in PTL.

There is strong evidence to suggest that intrauterine (IU) infection or inflammation has a strong association with preterm delivery (3,9–11). It is estimated that an overt or sub-clinical IU inflammation is present in close to 25–75% of births that result from spontaneous PTL (12,13). The timing of

onset of IU inflammation and whether these markers of inflammation are present in the plasma is unknown. A sensitive diagnostic marker identified in early pregnancy may assist in early application of preventive therapies for women at risk for developing PTL.

Surface-enhanced laser desorption/ionization time-of-flight mass spectrometry (SELDI-TOF/MS) is a high throughput proteomics technology that has been used for discovery of potential biomarkers of diseases (14–22).

In this study, we used a mouse model of inflammation-induced PTL to discover potential biomarkers that are differentially expressed between mice that delivered preterm vs. those that delivered at term.

MATERIALS AND METHODS

Animals. CD-1 mice, 8–10 wk old, were purchased from Charles River (Wilmington, MA). All animal protocols were performed in accordance with Stanford University Animal Care and Use Committee guidelines.

Experiment 1. Lipopolysaccharide (LPS) from *Escherichia coli* 0111:B4 purified by phenol extraction was used to induce IU inflammation (L2630, Sigma-Aldrich Chemical Co., St. Louis, MO). On d 14.5 of gestation, a mini laparotomy was performed, after anesthetizing with Avertin (240 mg/kg body weight). LPS (25 μ g) ($n = 10$) suspended in 100 μ L of PBS was injected between the first two gestational sacs of the right uterine horn using the technique described by Elovitz *et al.* (23). Control animals ($n = 10$) received 100 μ L of sterile PBS. After the uterus was returned to the abdomen, the fascia and the skin were closed. Using this method, the animals recovered well with no signs of morbidity.

Experiment 2. In the second series of experiments, all animals were injected with a lower dose of LPS. Twenty micrograms of LPS suspended in 100 μ L of PBS was injected between the first two gestational sacs of the right uterine horn on d 14.5 of gestation. Thirteen animals were injected.

Plasma collection. Blood samples were collected in an EDTA-coated microtainer (BD, Franklin Lakes, NJ) by infraorbital puncture and centrifuged at 5000 \times g for 10 min at 4°C. Plasma was removed, aliquoted, and stored at –80°C until analysis.

SELDI-TOF MS. The SELDI-TOF/MS protocol used for proteomics profiling has been described previously (24). Plasma (20 μ L) was pretreated with U9 solution (9 M urea/2% CHAPS/50 mM Tris pH 9; 30 μ L) and applied to a strong anion exchange bead at pH 9 (Q-ceramic HyperD F, Pall Life Sciences, Ann Arbor, MI) in a 96-well Silent Screen filtration plate (NUNC, Rochester, NY). The sample-loaded anion exchange beads were then washed sequentially with buffers (200 μ L each) at pH 9, 7, 5, 4, and 3, and finally with 33.3% isopropanol/16.7% acetonitrile (ACN)/50% H₂O/0.2% trifluoroacetic acid (TFA). Aliquots of the eluates (10 μ L each) from the above fractions were suspended in the appropriate binding buffers and applied to ProteinChip SELDI arrays: CM10, a weak cation-exchange surface and H50, a reversed-phase surface (Bio-Rad Laboratories, Hercules, CA). Binding buffers were 0.1 M sodium

Received November 13, 2008; accepted February 6, 2009.
Correspondence: Ashima Madan, M.D., S-4245A CCSR Building, 269 Campus Dr, Stanford, CA 94305-5178; e-mail: ashima@stanford.edu
Supported by the Hess (A.M.), Euphrates (H.J.C.), and Pediatric Research Funds (A.M.).

Abbreviations: ACN, acetonitrile; FDR, false discovery rate; IU, intrauterine; LPS, lipopolysaccharide; MW, Mann-Whitney; PTL, preterm labor; SAA, serum amyloid A; SELDI-TOF/MS, surface-enhanced laser desorption/ionization time-of-flight mass spectrometry; TFA, trifluoroacetic acid

acetate buffer (pH 4) for CM10 arrays and 10% ACN/0.1% TFA for H50 arrays. After washing and air drying, sinapinic acid was applied to the arrays.

The ProteinChip Arrays were read on a Bio-Rad PCS4000 mass spectrometer to obtain mass spectra of the fractionated samples. Mass spectra were obtained at three laser intensities: low (3500 nJ), medium (4800 nJ), and high (7250 nJ), using instrument parameters optimized for small, medium, and large proteins. A total of 60 spectra were generated for each sample (five fractions on two types of arrays with three different laser intensities run in duplicate). Spectra were externally calibrated using spectra of a mixture of protein standards in the range of 7–30 kDa (Protein Standards II, Bio-Rad).

Statistical analysis. All mass spectra were normalized by total ion current. Peak selection was based on m/z and signal intensity using the ProteinChip Data Manager Software 3.0.7, Enterprise Edition (Bio-Rad). The mean intensity for each peak from duplicate spectra was combined.

The Mann-Whitney U test was used to discover peaks discriminating between the PBS-injected control and LPS-injected study groups. To control for “multiple hypothesis testing” a permutation-based approach for the false discovery rate (FDR) estimation was used (25,26). When a given p value threshold was applied to the original data set to evaluate the significance of all peaks, the total number of differential peaks consisting of true and false positives was obtained. The same p value threshold when applied to all 100 permuted data sets yielded 100 different numbers of positive differential peaks.

The ratios between the false positives, including the mean, median, and 95% distribution of the 100 different false positives and total number of positives was used for the estimation of the FDR. After a global assessment of FDR, the local FDR was computed and used as an additional guideline for choosing the optimized p value threshold and deciding whether a peak was truly differentially expressed (27,28). The same method was used for spectra from experiment 2.

Biomarkers purification and identification. The three 11 kDa protein peaks that were significantly different between the PBS and LPS groups were further purified. Twenty microliters of plasma from LPS-injected mice was used. In the initial step, the ProteomeLab IgY-HSA SC Proteome Partitioning Kit (Beckman Coulter, Fullerton, CA) was used to remove abundant albumin in plasma. Flow through (500 μ L) was concentrated to 100 μ L using Microcon YM-3 Centrifugal Filter Unit (Millipore, Billerica, MA). Fractionation by anion-exchange chromatography was performed as described earlier (SELDI-TOF/MS). The concentrated flow through was washed sequentially with buffers (500 μ L each) at pH 7, 5, 4 and organic buffer. Each elution was detected on the CM10 chip by SELDI-TOF/MS.

Further purification using hydrophobic fractionation was performed as follows. Fractions 3 and 4 containing the protein peaks of interest were bound to reverse-phase beads (polystyrene/divinyl benzene PLRP-S beads, Polymer Laboratories, Amherst, MA) for 30 min at room temperature. The beads were centrifuged and the supernatant solution was collected after centrifugation. The protein bound beads were washed with solutions containing increasing percentages of ACN (10, 20, 30, 40, 50, 60, and 70%) in 0.1% TFA. Each hydrophobic fraction was collected and analyzed on NP20 array to locate the fractions containing the biomarker peaks.

Biomarkers were identified by 1-D SDS PAGE and MALDI-TOF/TOF-MS (Applied Biosystems 4700, Foster City, CA). Hydrophobic fractions containing the protein peaks of interest were dried and resuspended in SDS-PAGE sample buffer and run on a NuPAGE Bis-Tris gel (4–12%; Invitrogen, Carlsbad, CA). The gel was stained with Coomassie Blue (SimplyBlue, Invitrogen) followed by destaining overnight at 4°C. Bands at approximately 11 kDa were excised. Protein was extracted from part of the gel pieces using 10 μ L of an elution buffer (50% formic acid, 25% ACN, 15% 2-propanol, and 10% water) and the bands containing the biomarker peaks were identified by obtaining mass spectra of the gel band extracts on NP20 ProteinChip arrays.

Each gel piece containing the biomarker peak was reduced with DTT, alkylated with iodoacetamide, and digested with 100 ng trypsin. Trypsin digests were spotted to MALDI target plates and analyzed by MALDI-TOF/TOF MS. The 10 most abundant ions that did not correspond to the known masses of trypsin autolytic products were analyzed by MS/MS to obtain sequence data. The Mascot search engine was used to search the NCBI database for protein identification.

ELISA assay. Serum amyloid A (SAA) 2 levels in mouse plasma were measured using an ELISA kit specific for mouse SAA2 (Life Diagnostics Inc. West Chester, PA). Standards and samples were tested in duplicate.

RESULTS

Experiment 1. In the initial dose-response series conducted before sample collection for SELDI-TOF/MS, IU injection of 25 μ g LPS resulted in PTL in 10 of 11 injected mice. This

dose was subsequently used for studies in experiment 1. Plasma of all mice was sampled 15 h after LPS ($n = 10$) or PBS injection ($n = 10$) and processed for MS to find biomarkers associated with LPS-induced prematurity. Peaks were obtained after mass calibration, baseline subtraction, and normalization using the clustering and alignment function of ProteinChip Data Manager Software 3.0.7, Enterprise Edition. Altogether, 1665 peaks were evaluated by the Mann-Whitney U test. Of these peaks, 222 were significantly different at $p < 0.01$, 100 at $p < 0.001$, and 30 at $p < 0.0001$ (data not shown).

One method to control for the number of statistical tests being performed (a problem of multiple hypothesis testing) is to examine the FDR for these data. The web-based FDR analysis tool (<http://translationalmedicine.stanford.edu/Mass-Conductor/FDR.html>, Ling, unpublished data) was used to calculate the global FDR at different Mann-Whitney p value thresholds and the protein-specific local FDR (27,28). To select a stringent cutoff, the local FDR of 0.005 was used to guide the selection of the p value threshold, leading to a Mann-Whitney p value of 0.0001. At this threshold, global FDR has been controlled to be less than 0.1%. In summary, the selection of Mann-Whitney p value of 0.0001 as the optimized p value threshold, guided by both the global and local FDR analysis yielded a total of 30 highly differentially expressed peaks for further characterization.

Experiment 2. The goal in experiment 2 was to inject all mice with a slightly lower concentration of LPS, a concentration that would not lead to premature birth in all the mice. Injection of 13 mice with the lower concentration of LPS resulted in seven mice that delivered at term, and six mice that gave birth preterm. When the plasma samples were analyzed, a total of 1718 peaks were detected. There were 128 peaks with p value < 0.01 with FDR < 0.1 (data not shown).

The most significantly different peaks in both experiments were a group of m/z 11,600–11,800 found in fractions 3 and 4 of the anion-exchange-treated plasma samples. On the basis of the results from FDR, p values, ROC, and spectra from experiments 1 (Table 1) and 2 (Table 2), three biomarker peaks with m/z of approximately 11,640, 11,720, and 11,780 (Fig. 1) were further purified and identified.

Biomarker identification. After depletion of albumin, mouse plasma was fractionated on anion-exchange chromatography similar to that used during the discovery phase. The material that eluted from anion-exchange beads in fraction 4 (a pH 4 extraction that followed a pH 5 extraction) was further fractionated by reverse-phase chromatography. The material that eluted at 40% ACN was dried, solubilized in SDS-PAGE buffer, and separated using SDS-PAGE. As shown in Figure 2C, bands A and B from SDS-PAGE were found at approximately 11 kDa, which was close to the m/z 11,600–11,800 biomarkers detected by SELDI. Protein extracted from both bands A and B was confirmed by SELDI using the NP20 chip. Figure 2A, B, D, and E shows the mass spectra obtained during the purification process. A peak with mass size 11,899 was detected from band A (Fig. 2D) and two peaks 11,792 and 11,875 were detected from band B (Fig. 2E). Other portions of these bands were digested with trypsin, and the resultant material was analyzed by MALDI-MS/MS. Sequence analysis demonstrated that each 11 kDa band

Table 1. Proteomic features expressed significantly between LPS-injected and PBS-injected groups with $p < 0.0001$ and local FDR < 0.005

Feature	SELDI surface-fraction-laser	Peak (m/z)	ROC	Local FDR	p	Intensity \pm SD		Fold change
						PBS ($n = 10$)	LPS ($n = 10$)	
1	CM10-Fx3-medium	11,643	0.98	0.00147	0.0000108	6.3 \pm 5.8	53.5 \pm 30.8	8.49
	H50-Fx3-medium	11,637	0.98	0.00391	0.0000433	23.6 \pm 31.9	218.2 \pm 119.2	9.25
	H50-Fx3-low	5,818	0.98	0.00391	0.0000433	3.5 \pm 3.6	25.4 \pm 17.2	7.26
	H50-Fx3-medium	5,814	0.98	0.00168	0.0000217	4.6 \pm 4.9	33.9 \pm 18.4	7.37
2	CM10-Fx3-medium	11,722	0.98	0.00391	0.0000433	11.2 \pm 4.6	32.9 \pm 13.8	2.94
	H50-Fx3-medium	11,769	0.98	0.00168	0.0000217	18.5 \pm 23.0	170.3 \pm 92.4	9.21
	H50-Fx4-medium	11,754	0.94	0.00391	0.0000758	19.3 \pm 23.1	121.2 \pm 77.1	6.28
3	CM10-Fx3-medium	11,789	0.98	0.00147	0.0000108	7.4 \pm 6.6	64.1 \pm 37.9	8.66
	H50-Fx3-medium	11,867	0.98	0.00391	0.0000433	4.8 \pm 6.0	41.2 \pm 25.0	8.58
	CM10-Fx3-low	5,883	0.98	0.00147	0.0000108	1.6 \pm 0.5	5.7 \pm 3.8	3.56
	CM10-Fx3-medium	5,886	0.98	0.00147	0.0000108	1.8 \pm 1.8	10.2 \pm 4.7	5.67
	H50-Fx3-medium	5,899	0.98	0.00147	0.0000108	5.8 \pm 3.4	28.6 \pm 15.1	4.93
	H50-Fx3-low	5,903	0.98	0.00147	0.0000108	4.1 \pm 2.4	20.8 \pm 12.9	5.07
4	H50-Fx5-medium	5,905	0.94	0.00391	0.0000758	1.1 \pm 0.7	3.8 \pm 1.6	3.45
	CM10-Fx3-medium	11,979	0.98	0.00391	0.0000217	3.4 \pm 2.4	17.8 \pm 10.5	5.24
	H50-Fx4-medium	11,990	0.94	0.00391	0.0000758	3.1 \pm 3.5	17.6 \pm 10.5	5.68
	H50-Fx3-medium	11,995	0.98	0.00168	0.0000217	3.0 \pm 3.4	26.3 \pm 14.7	8.77
5	CM10-Fx3-medium	12,163	0.94	0.00391	0.0000758	2.2 \pm 1.7	10.1 \pm 5.5	4.59
	H50-Fx3-medium	12,171	0.98	0.00147	0.0000108	0.9 \pm 0.4	4.8 \pm 2.6	5.33
	H50-Fx4-medium	12,245	0.98	0.00391	0.0000108	1.2 \pm 0.8	4.8 \pm 2.5	4.00
6	CM10-Fx3-medium	12,336	0.94	0.00168	0.0000758	1.0 \pm 1.0	6.2 \pm 3.6	6.20
	H50-Fx3-medium	12,430	0.94	0.00391	0.0000758	0.4 \pm 0.4	2.8 \pm 1.6	8.23
7	H50-Fx3-high	20,309	0.98	0.00168	0.0000217	0.1 \pm 0.01	0.5 \pm 0.2	6.27
	H50-Fx3-medium	20,389	0.98	0.00391	0.0000433	0.2 \pm 0.1	0.7 \pm 0.3	4.23
8	H50-Fx3-medium	20,528	0.98	0.00168	0.0000217	0.1 \pm 0.1	0.7 \pm 0.3	4.85
9	CM10-Fx3-high	28,145	0.94	0.00391	0.0000758	5.2 \pm 2.0	11.8 \pm 3.9	2.27
10	H50-Fx3-high	39,900	0.98	0.00168	0.0000217	0.2 \pm 0.1	0.6 \pm 0.2	2.81
	H50-Fx1-high	79,796	0.98	0.00391	0.0000758	0.02 \pm 0.01	0.04 \pm 0.01	1.64

p values were from Mann-Whitney U test.

contained a mixture of mouse SAA1 and 2 as showed in Figure 2F and G. The presence of two SAA isoforms in each band is demonstrated by the observation of SAA1-derived peptides of masses 1130.50 and 1455.62 (indicated in boxes in Fig. 2F and G) and peptides of masses 1146.50 and 1487.73 (underlined in Fig. 2F and G) in the MS spectra of both bands.

The mass of mouse SAA1 is 11,754, and that of mouse SAA2 is 11,605. There is a shift in m/z of the peaks extracted from SDS-PAGE from both the m/z of the biomarkers before SDS-PAGE, and the calculated mass of the proteins of the peptides identified in the SDS-PAGE gel bands. This shift is likely due to a combination of modifications of proteins that occur during SDS-PAGE (e.g. alkylation with acrylamide adds 71 to the mass) and extraction of proteins from SDS-PAGE gel bands (e.g. multiple formylation reactions, each of which adds 28 to the mass) (29,30).

ELISA. In experiment 1, the median and mean plasma levels of SAA2 were elevated 40-fold and 10-fold, respectively in the LPS-treated animals compared with PBS controls (Table 3). In experiment 2, the median and mean SAA 2 levels were 2-fold higher in the mice that delivered preterm compared with those that delivered at term (Table 4).

DISCUSSION

In the first series of studies, we found several biomarkers that were significantly different between control mice that delivered at term and LPS-treated mice that developed PTL. In the second series of studies, in which mice were injected with

a lower dose of LPS, some developed PTL, whereas others injected with the same dose delivered at term. There were several differences in the biomarker profiles between these two groups. Of the two biomarkers that were different between the animals that delivered at term vs. preterm, we identified two 11 kDa biomarkers to be SAA1 and SAA2.

SAA has been identified as a plasma biomarker in several disease states including prostate and ovarian cancer (31–33). Quantitative analysis by ELISA showed that the amount of SAA2 was higher in animals that developed PTL vs. term labor in both groups, validating the role of SAA in the development of PTL in this model. Despite the small sample size of this study, the results are intriguing.

The SAA family includes several proteins with a molecular weight between 11 and 12 kDa (34). SAA is an acute phase reactant that is generated largely by the liver, but also in leukocytes and by other organs (35). High amounts are present in inflammatory disorders such as rheumatoid arthritis, atherosclerosis, and in various malignant diseases (36–38). It has also been shown to be present in the human first trimester trophoblast (39).

It has been hypothesized that in PTL, infection or inflammation results in the release of proinflammatory cytokines that stimulate matrix metalloproteases (MMPs) and prostaglandin synthesis resulting in uterine contractions (40,41). The regulation of SAA gene expression occurs at the level of transcription. Although there are various pathways and transcription factors that can activate SAA expression under different conditions, SAA gene expression in inflammation is induced by

Table 2. Proteomic features expressed significantly between LPS-injected groups that delivered preterm vs. term with $p < 0.05$

Feature	SELDI surface-fraction-laser	Peak (m/z)	ROC	p	Intensity \pm SD		Fold change
					LPS-term ($n = 7$)	LPS-preterm ($n = 6$)	
1	CM10-Fx3-medium	5,813	0.89	0.014	4.8 \pm 2.6	11.6 \pm 4.5	2.42
	CM10-Fx3-medium	11,637	0.94	0.0082	49.1 \pm 24.9	101.9 \pm 23.7	2.08
	CM10-Fx4-medium	11,635	0.79	0.035	113.8 \pm 34.9	154.8 \pm 33.6	1.36
	CM10-Fx5-medium	5,820	0.85	0.035	154.7 \pm 38.9	209.9 \pm 46.0	1.46
	CM10-Fx6-medium	11,643	0.79	0.014	19.6 \pm 6.3	30.4 \pm 10.2	1.55
		5,821	0.85	0.0221	111.6 \pm 35.3	180.3 \pm 43.3	1.62
	H50-Fx3-low	5,819	0.94	0.0082	6.7 \pm 4.2	20.5 \pm 7.8	3.06
	H50-Fx3-medium	5,817	0.94	0.0082	10.1 \pm 5.3	23.8 \pm 7.5	2.36
		11,646	0.94	0.0082	57.1 \pm 48.3	147.3 \pm 39.8	2.58
	H50-Fx4-low	5,819	0.89	0.0221	8.1 \pm 2.7	14.3 \pm 4.1	1.77
	H50-Fx4-medium	11,621	0.94	0.0047	4.3 \pm 4.0	19.3 \pm 10.2	4.49
		5,814	0.89	0.0221	12.7 \pm 3.7	21.1 \pm 5.8	1.67
	H50-Fx6-medium	11,645	0.89	0.0221	10.2 \pm 3.9	17.1 \pm 4.0	1.68
	2	CM10-Fx3-medium	11,723	0.85	0.035	42.4 \pm 14.4	65.3 \pm 16.3
CM10-Fx4-medium		5,865	0.94	0.0047	47.1 \pm 12.9	71.1 \pm 7.4	1.51
3		11,722	0.89	0.014	75.3 \pm 20.1	103.1 \pm 19.8	1.37
	CM10-Fx3-low	5,878	0.94	0.0082	5.0 \pm 2.6	12.6 \pm 4.5	2.52
	CM10-Fx3-medium	5,878	0.94	0.0082	8.5 \pm 3.3	15.9 \pm 4.3	1.87
		11,784	0.94	0.0082	56.6 \pm 27.3	124.1 \pm 35.3	2.19
	CM10-Fx4-medium	5,886	0.85	0.014	37.1 \pm 12.2	56.6 \pm 11.3	1.53
		11,781	0.85	0.0221	160.9 \pm 53.6	223.7 \pm 55.3	1.39
	CM10-Fx6-medium	11,782	0.85	0.0221	44.2 \pm 15.5	65.1 \pm 18.1	1.47
	H50-Fx3-low	5,899	0.94	0.0082	5.7 \pm 3.0	18.2 \pm 8.0	3.79
	H50-Fx3-medium	5,897	0.94	0.0082	8.8 \pm 3.4	21.5 \pm 7.3	2.44
		11,783	0.94	0.0082	47.9 \pm 23.4	138.5 \pm 49.4	2.89
	H50-Fx4-low	5,899	0.85	0.035	9.4 \pm 3.1	17.4 \pm 5.7	1.85
	H50-Fx4-low	5,899	0.94	0.0082	14.7 \pm 3.8	24.9 \pm 6.9	1.69
		11,779	0.85	0.014	79.6 \pm 23.2	150.1 \pm 44.7	1.89
	H50-Fx5-low	5,897	0.94	0.0082	14.7 \pm 3.8	24.9 \pm 6.9	1.69
H50-Fx5-medium	5,898	0.85	0.0221	3.8 \pm 1.1	5.5 \pm 1.3	1.45	
	11,783	0.85	0.0221	14.4 \pm 4.9	22.1 \pm 6.3	1.53	
H50-Fx6-medium	11,781	0.89	0.035	13.2 \pm 5.0	21.7 \pm 4.7	1.64	
4	CM10-Fx3-medium	11,992	0.94	0.0082	12.3 \pm 5.0	25.2 \pm 8.0	2.02
	H50-Fx3-low	5,987	0.94	0.0082	1.7 \pm 0.8	4.9 \pm 2.1	2.88
	H50-Fx3-medium	5,984	0.89	0.0082	4.4 \pm 0.5	5.3 \pm 0.4	1.20
		11,993	0.94	0.0082	7.9 \pm 3.5	21.3 \pm 7.4	2.67
	H50-Fx4-medium	11,994	0.85	0.0221	12.1 \pm 3.9	20.1 \pm 5.5	1.66
	H50-Fx5-medium	11,994	0.85	0.0221	3.0 \pm 1.0	4.6 \pm 1.3	1.53
	H50-Fx6-medium	11,996	0.89	0.014	2.4 \pm 0.9	3.8 \pm 0.8	1.58

p values were from Mann-Whitney U test.

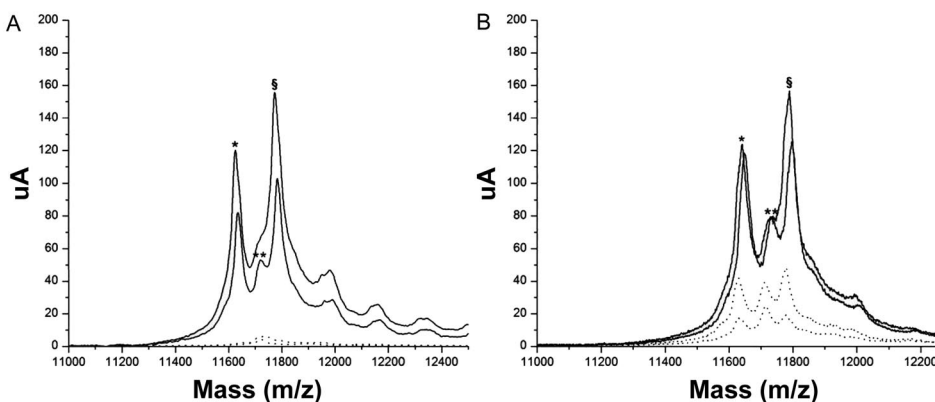


Figure 1. Representative SELDI spectra from plasma. (A) Group of peaks of m/z 11,600–11,800 on CM10 chips from experiment 1. The three peaks 11.63 (*), 11.72 (**), and 11.78 (§) kDa are shown. Plasma spectra from mice injected with 25 μ g LPS (solid line) or PBS (dotted line). (B) Group of peaks of m/z 11,600–11,800 on CM10 chips from experiment 2. Plasma spectra from mice injected with 20 μ g LPS that delivered preterm (solid line) or term (dotted line).

various proinflammatory cytokines (42). In turn, SAA can induce secretion of cytokines by leukocytes and stimulate attraction of leukocytes in areas of inflammation, thus augmenting the cycle (43,44). SAA also induces expression of

MMPs, enzymes degrading extracellular matrix (45), a key step in cervical ripening during labor.

LPS, a major component of the outer wall of Gram-negative bacteria acts by binding to adaptor proteins which allow for

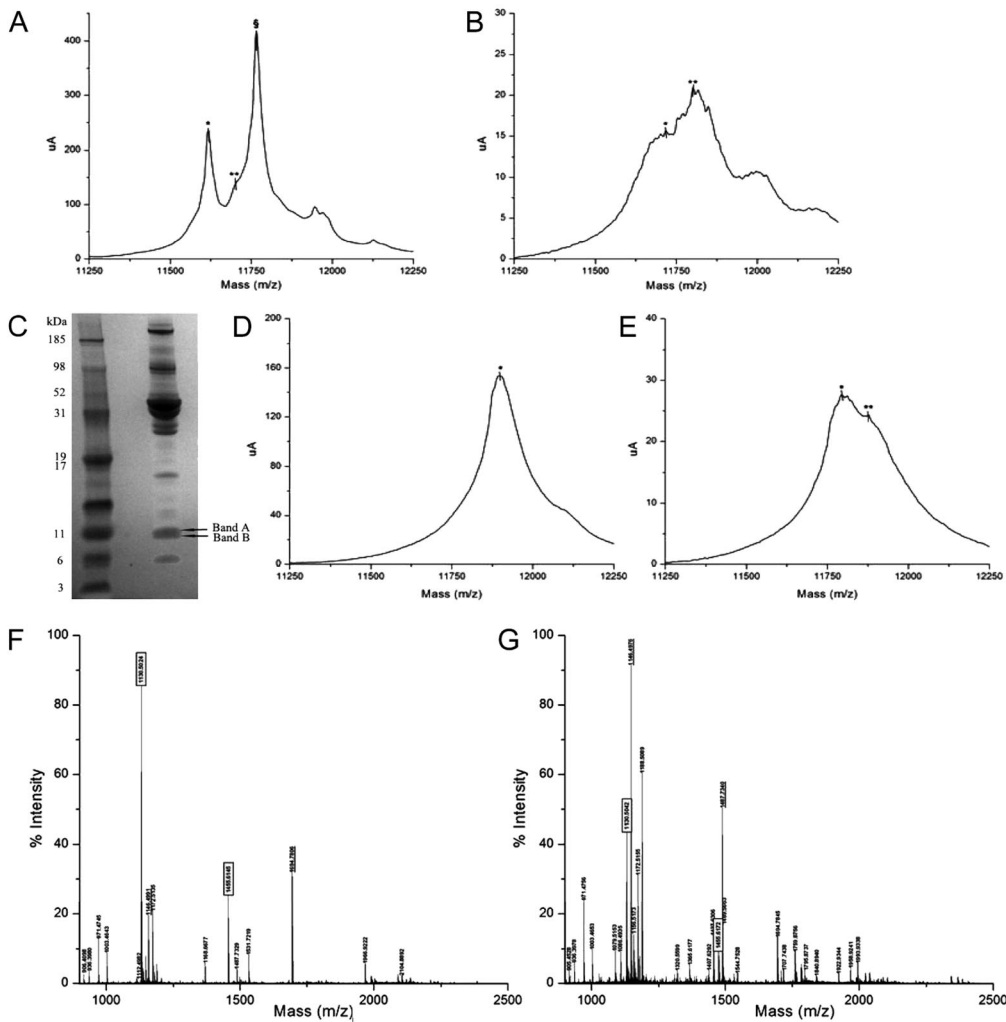


Figure 2. Identification of biomarkers SAA1 and SAA2. (A–E) SELDI-TOF spectra of biomarker during purification. (A) Spectrum of the biomarkers in fraction 4 on CM10 arrays. Mass (*m/z*) of peaks are 11,616.92 (*), 11,713.20 (**), and 11,765.86 (§). (B) Spectrum of the 40% ACN fraction from reverse phase beads of fraction 4. Mass (*m/z*) of peaks are 11,712.43 (*) and 11,808.95 (**). (C) Proteins in 40% ACN fraction separated using SDS-PAGE. Biomarkers (bands A and B) located close to 11 kDa. (D and E) Spectra of proteins extracted from the 11 kDa bands (bands A and B) after SDS-PAGE of the 40% ACN fraction, respectively. Mass (*m/z*) of peaks are 11,898.66 (*) in D and 11,792.35 (*) and 11,875.25 (**) in E. (F and G) Sequence analysis of trypsin-digested proteins extracted from bands A and B. The peaks indicated by the boxes are for peptides derived from SAA1, and the peaks underlined are peptides derived from SAA2.

Table 3. Plasma concentration of SAA2 in mouse model of preterm birth (experiment 1)

Group	Median (range)	Mean ± SD	<i>p</i>
PBS (<i>n</i> = 8)	12.3 (0.4–320.3)	78.1 ± 121.9	0.0089
LPS (<i>n</i> = 10)	487.4 (222.3–2254.3)	722.2 ± 611.7	

Values are in μg/mL and expressed as mean ± SD and median (range); *n* means numbers of samples, which was measured; *p* value was compared means between LPS-injected and PBS-injected groups using *t* test.

Table 4. Plasma concentration of SAA2 in mouse model of preterm birth (experiment 2)

Group	Median (range)	Mean ± SD	<i>p</i>
LPS-term (<i>n</i> = 5)	321.0 (278.9–344.6)	320.9 ± 29.3	0.039
LPS-preterm (<i>n</i> = 5)	617.9 (412.6–836.6)	621.2 ± 173.7	

Values are in μg/mL and expressed as mean ± SD and median (range); *n* means numbers of samples, which was measured; *p* value was compared means between LPS-induced preterm and LPS-term groups using *t* test.

binding to toll-like receptor-4 (46). This results in activation of a pathway leading to activation of NF-κB and upregulation of various proinflammatory cytokines. These cytokines stimulate SAA production with further augmentation of the inflammatory cascade resulting ultimately in premature uterine contractions.

We hypothesize that SAA plays an important role in the pathogenesis of inflammation-induced PTL, and can possibly serve as a biomarker of inflammation-induced PTL early in pregnancy. SAA levels have been shown to be increased in pregnant women with preeclampsia compared with controls (47). Although the animal model used was not optimal for the study of preeclampsia or IU growth retardation, conditions that are associated with PTL, it is interesting to speculate if SAA may be a marker for other obstetrical complications that result in premature delivery. Because of inherent differences between mouse and human pregnancies, extrapolating these findings to the bedside is fraught with difficulties. Further studies in both animal models and humans will need to be performed to determine the clinical significance of these findings.

REFERENCES

- Slattery MM, Morrison JJ 2002 Preterm delivery. *Lancet* 360:1489–1497
- Lemons JA, Bauer CR, Oh W, Korones SB, Papile LA, Stoll BJ, Verter J, Temprosa M, Wright LL, Ehrenkranz RA, Fanaroff AA, Stark A, Carlo W, Tyson JE, Donovan EF, Shankaran S, Stevenson DK 2001 Very low birth weight outcomes of the National Institute of Child health and human development neonatal research network, January 1995 through December 1996. *NICHD Neonatal Research Network. Pediatrics* 107:E1
- Goldenberg RL, Hauth JC, Andrews WW 2000 Intrauterine infection and preterm delivery. *N Engl J Med* 342:1500–1507
- Simhan HN, Caritis SN 2007 Prevention of preterm delivery. *N Engl J Med* 357:477–487
- Smith R 2007 Parturition. *N Engl J Med* 356:271–283

6. Meis PJ, Klebanoff M, Thom E, Dombrowski MP, Sibai B, Moawad AH, Spong CY, Hauth JC, Miodovnik M, Varner MW, Leveno KJ, Caritis SN, Iams JD, Wapner RJ, Conway D, O'Sullivan MJ, Carpenter M, Mercer B, Ramin SM, Thorp JM, Peaceman AM, Gabbe S 2003 Prevention of recurrent preterm delivery by 17 alpha-hydroxyprogesterone caproate. *N Engl J Med* 348:2379–2385
7. Fonseca EB, Celik E, Parra M, Singh M, Nicolaides KH 2007 Progesterone and the risk of preterm birth among women with a short cervix. *N Engl J Med* 357:462–469
8. Goldenberg RL, Goepfert AR, Ramsey PS 2005 Biochemical markers for the prediction of preterm birth. *Am J Obstet Gynecol* 192:S36–S46
9. Goldenberg RL, Culhane JF 2003 Infection as a cause of preterm birth. *Clin Perinatol* 30:677–700
10. Goncalves LF, Chaiworapongsa T, Romero R 2002 Intrauterine infection and prematurity. *Ment Retard Dev Disabil Res Rev* 8:3–13
11. Christiaens I, Zaragoza DB, Guilbert L, Robertson SA, Mitchell BF, Olson DM 2008 Inflammatory processes in preterm and term parturition. *J Reprod Immunol* 79:50–57
12. Pennell CE, Jacobsson B, Williams SM, Buus RM, Muglia LJ, Dolan SM, Morken NH, Ozcelik H, Lye SJ, Relton C 2007 Genetic epidemiologic studies of preterm birth: guidelines for research. *Am J Obstet Gynecol* 196:107–118
13. Gibbs RS, Romero R, Hillier SL, Eschenbach DA, Sweet RL 1992 A review of premature birth and subclinical infection. *Am J Obstet Gynecol* 166:1515–1528
14. Petricoin EF, Ardekani AM, Hitt BA, Levine PJ, Fusaro VA, Steinberg SM, Mills GB, Simone C, Fishman DA, Kohn EC, Liotta LA 2002 Use of proteomic patterns in serum to identify ovarian cancer. *Lancet* 359:572–577
15. Basso D, Valerio A, Seraglia R, Mazza S, Piva MG, Greco E, Fogar P, Gallo N, Pedrazzoli S, Tiengo A, Plebani M 2002 Putative pancreatic cancer-associated diabetogenic factor: 2030 MW peptide. *Pancreas* 24:8–14
16. Yasui Y, Pepe M, Thompson ML, Adam BL, Wright GL Jr, Qu Y, Potter JD, Winget M, Thornquist M, Feng Z 2003 A data-analytic strategy for protein biomarker discovery: profiling of high-dimensional proteomic data for cancer detection. *Bio-statistics* 4:449–463
17. Clarke W, Silverman BC, Zhang Z, Chan DW, Klein AS, Molmenti EP 2003 Characterization of renal allograft rejection by urinary proteomic analysis. *Ann Surg* 237:660–664; discussion 664–665
18. Poon TC, Hui AY, Chan HL, Ang IL, Chow SM, Wong N, Sung JJ 2005 Prediction of liver fibrosis and cirrhosis in chronic hepatitis B infection by serum proteomic fingerprinting: a pilot study. *Clin Chem* 51:328–335
19. Conrads TP, Fusaro VA, Ross S, Johann D, Rajapakse V, Hitt BA, Steinberg SM, Kohn EC, Fishman DA, Whitely G, Barrett JC, Liotta LA, Petricoin EF III, Veenstra TD 2004 High-resolution serum proteomic features for ovarian cancer detection. *Endocr Relat Cancer* 11:163–178
20. Rubin RB, Merchant M 2000 A rapid protein profiling system that speeds study of cancer and other diseases. *Am Clin Lab* 19:28–29
21. Wagner M, Naik DN, Pothan A, Kasukurti S, Devineni RR, Adam BL, Semmes OJ, Wright GL Jr 2004 Computational protein biomarker prediction: a case study for prostate cancer. *BMC Bioinformatics* 5:26
22. Gravett MG, Novy MJ, Rosenfeld RG, Reddy AP, Jacob T, Turner M, McCormack A, Lapidus JA, Hitti J, Eschenbach DA, Roberts CT Jr, Nagalla SR 2004 Diagnosis of intra-amniotic infection by proteomic profiling and identification of novel biomarkers. *JAMA* 292:462–469
23. Elovitz MA, Wang Z, Chien EK, Rychlik DF, Phillippe M 2003 A new model for inflammation-induced preterm birth: the role of platelet-activating factor and Toll-like receptor-4. *Am J Pathol* 163:2103–2111
24. Madan A, El-Ferzli G, Carlson SM, Whittin JC, Schilling J, Najmi A, Yu TT, Lau K, Dimmitt RA, Cohen HJ 2007 A potential biomarker in the cord blood of preterm infants who develop retinopathy of prematurity. *Pediatr Res* 61:215–221
25. Benjamini Y, Hochberg Y 1995 Controlling the false discovery rate: a practical and powerful approach to multiple testing. *J Roy Statist Soc Ser B* 57:289–300
26. Tusher VG, Tibshirani R, Chu G 2001 Significance analysis of microarrays applied to the ionizing radiation response. *Proc Natl Acad Sci USA* 98:5116–5121
27. Efron B, Tibshirani R 2002 Empirical Bayes methods and false discovery rates for microarrays. *Genet Epidemiol* 23:70–86
28. Aubert J, Bar-Hen A, Daudin JJ, Robin S 2004 Determination of the differentially expressed genes in microarray experiments using local FDR. *BMC Bioinformatics* 5:125
29. Galvani M, Bordini E, Piubelli C, Hamdan M 2000 Effect of experimental conditions on the analysis of sodium dodecyl sulphate polyacrylamide gel electrophoresis separated proteins by matrix-assisted laser desorption/ionisation mass spectrometry. *Rapid Commun Mass Spectrom* 14:18–25
30. Hamdan M, Galvani M, Righetti PG 2001 Monitoring 2-D gel-induced modifications of proteins by MALDI-TOF mass spectrometry. *Mass Spectrom Rev* 20:121–141
31. Le L, Chi K, Tyldesley S, Flibotte S, Diamond DL, Kuzyk MA, Sadar MD 2005 Identification of serum amyloid A as a biomarker to distinguish prostate cancer patients with bone lesions. *Clin Chem* 51:695–707
32. Li Y, Dang TA, Shen J, Perlaky L, Hicks J, Murray J, Meyer W, Chintagumpala M, Lau CC, Man TK 2006 Identification of a plasma proteomic signature to distinguish pediatric osteosarcoma from benign osteochondroma. *Proteomics* 6:3426–3435
33. Moshkovskii SA, Serebryakova MV, Kuteykin-Teplyakov KB, Tikhonova OV, Goufman EI, Zgoda VG, Taranets IN, Makarov OV, Archakov AI 2005 Ovarian cancer marker of 11.7 kDa detected by proteomics is a serum amyloid A1. *Proteomics* 5:3790–3797
34. Uhlir CM, Whitehead AS 1999 Serum amyloid A, the major vertebrate acute-phase reactant. *Eur J Biochem* 265:501–523
35. Urieli-Shoval S, Cohen P, Eisenberg S, Matzner Y 1998 Widespread expression of serum amyloid A in histologically normal human tissues. Predominant localization to the epithelium. *J Histochem Cytochem* 46:1377–1384
36. O'Hara R, Murphy EP, Whitehead AS, FitzGerald O, Bresnihan B 2000 Acute-phase serum amyloid A production by rheumatoid arthritis synovial tissue. *Arthritis Res* 2:142–144
37. Meek RL, Urieli-Shoval S, Benditt EP 1994 Expression of apolipoprotein serum amyloid A mRNA in human atherosclerotic lesions and cultured vascular cells: implications for serum amyloid A function. *Proc Natl Acad Sci USA* 91:3186–3190
38. Vlasova MA, Moshkovskii SA 2006 Molecular interactions of acute phase serum amyloid A: possible involvement in carcinogenesis. *Biochemistry (Mosc)* 71:1051–1059
39. Kovacevic A, Hammer A, Sundl M, Pfister B, Hrzenjak A, Ray A, Ray BK, Sattler W, Malle E 2006 Expression of serum amyloid A transcripts in human trophoblast and fetal-derived trophoblast-like choriocarcinoma cells. *FEBS Lett* 580:161–167
40. Baggia S, Gravett MG, Witkin SS, Haluska GJ, Novy MJ 1996 Interleukin-1 beta intra-amniotic infusion induces tumor necrosis factor-alpha, prostaglandin production, and preterm contractions in pregnant rhesus monkeys. *J Soc Gynecol Invest* 3:121–126
41. Brown NL, Alvi SA, Elder MG, Bennett PR, Sullivan MH 1998 A spontaneous induction of fetal membrane prostaglandin production precedes clinical labour. *J Endocrinol* 157:R1–R6
42. Hagihara K, Nishikawa T, Isobe T, Song J, Sugamata Y, Yoshizaki K 2004 IL-6 plays a critical role in the synergistic induction of human serum amyloid A (SAA) gene when stimulated with proinflammatory cytokines as analyzed with an SAA isoform real-time quantitative RT-PCR assay system. *Biochem Biophys Res Commun* 314:363–369
43. Badolato R, Wang JM, Murphy WJ, Lloyd AR, Michiel DF, Bausserman LL, Kelvin DJ, Oppenheim JJ 1994 Serum amyloid A is a chemoattractant: induction of migration, adhesion, and tissue infiltration of monocytes and polymorphonuclear leukocytes. *J Exp Med* 180:203–209
44. Patel H, Fellowes R, Coade S, Woo P 1998 Human serum amyloid A has cytokine-like properties. *Scand J Immunol* 48:410–418
45. Lee HY, Kim MK, Park KS, Bae YH, Yun J, Park JI, Kwak JY, Bae YS 2005 Serum amyloid A stimulates matrix-metalloproteinase-9 upregulation via formyl peptide receptor like-1-mediated signaling in human monocytic cells. *Biochem Biophys Res Commun* 330:989–998
46. Takeda K, Akira S 2003 Toll receptors and pathogen resistance. *Cell Microbiol* 5:143–153
47. Engin-Ustun Y, Ustun Y, Karabulut AB, Ozkaplan E, Meydanli MM, Kafkasli A 2007 Serum amyloid A levels are increased in pre-eclampsia. *Gynecol Obstet Invest* 64:117–120